MATHEMATICAL MODEL FOR THE TEMPERATURE DISTRIBUTION ON THE SURFACE OF TWO ALUMINUM ALLOYS WELDED BY FRICTION STIR WELDING

E. T. Karash[1], H. M. Ali[2], A. F. Hamid[3]

[1]Northern Technical University, Technical Institute Mosul, Iraq
[2, 3] Refrigeration Department, Technical College of Engineering, Northern Technical University, Mosul, Iraq
*Corresponding author's e-mail address: emadbane2007@ntu.edu.iq, alabadi.hussein@ntu.edu.iq, amina.hamed@ntu.edu.iq

ABSTRACT

The aim of this study was to predict the temperatures on all surfaces of three-dimensional models using the ANSYS 15.0 program. Firstly, the temperatures from the welding centre to the edges of the models of two aluminium alloys (AA-7075 & AA-2024) welded by friction stir welding process were perceived. Secondly, the distribution of temperatures from the start of the welding process to its end and the derivation of equations to predict the distribution of temperatures with the time spent in the welding process, along with the distribution of temperatures with the distance from the centre of the welding process were observed at different travel speeds of the welding cart (TS = 20, 40, 60, 100 mm/sec) and different speeds of the welding tool (TRS=900, 1050, 1200 rpm). The results indicate that the temperature increases with the increase in the rotational speed of the welding tool, while the temperature decreases with the increase in the travel speed of the welding cart. Another result is that the temperature distribution is not symmetrical. The highest values are in the welding centre and decrease significantly as the welding centre is moved away, and the highest temperatures can be reached between (75 – 80%) in the welding centre from the melting point of the two aluminium alloys welded together. It was also found that the temperatures increase significantly twenty seconds after the beginning of the welding process and, afterwards, the increase is small, and three equations were derived to predict the temperature distribution.

KEYWORDS: rotational speed, travel speed, aluminium alloys, friction stir welding, finite element analysis.

1. INTRODUCTION

Several practical and theoretical studies have been conducted for the process of friction stir welding, first for aluminum alloys, and then for welding different metals such as steel, copper, etc., as well as for welding polymers, because welding in this way has amazing mechanical specifications in industry and technology and in connecting metals to each other [1] - [4]. In many studies, the effect of variable factors such as the welding tool, the linear speed of the welding tool and the linear speed of the trolley carrying the model was studied. Sheets of different metals and alloys were used and different measurements were taken and used in the field of aviation and ships in different atmospheres and under different temperatures [5] - [10]. This process inherently produces a weld with lower stress and distortion compared to fusion welding methods, since there are no melting substances occur during welding [11]. This process has been widely used in many industries such as aerospace, aircraft, marine and transportation and food processing. This is because it produces low metal deformation, high quality, low residual stresses, fewer welding defects and low-cost joints, which are the main advantages of this method [12]. Finite element methods are also used to study the effect of FSW process parameters on the mechanical properties of different welded alloys based on solids mechanics [13] or mathematical model development [14]. Thus, a lot of research has been done to study the simulation of temperature distribution during friction stir welding processes. This was recognized in the current study based on the ANSYS software, and the results obtained from the simulation were compared with those of the actual experiment [15]. Finite element analysis is an effective method of welding investigation, because immediate results can be obtained. There is a group of researches that dealt with the study of the friction stir welding process.

Models were designed to study the temperature

Date of submission/acceptance: 01.06.2022/15.12.2022 https://doi.org/10.35219/awet.2022.04

distribution when friction stir welding two asymmetric aluminum alloys (AA2024- AA7075). The results of the study showed that increasing the speed of the welding tool leads to an increase in temperatures, but the results showed the opposite, as the temperatures decrease with the increase in the travel speed of the strip, and the results also showed a rise in the viscosity of the agitating area when the travel speed of the cart increased [16]. The researchers studied the effect of temperature distribution and heat input during friction stir welding. The temperatures were recorded from different positions in the direction of the thickness of the sample and perpendicular to the direction of movement of the pin tool during welding, under different welding conditions. It was found that the highest temperature in the welding line is less than 0.8Tm for these conditions. The temperature used in this work does not change significantly in the direction of the thickness of the sample. The temperature distribution perpendicular to the weld is approximately isothermal under the shoulder of the pin tool. The increase in welding pressure and the speed of rotation of the pin tool increase the maximum welding temperature. Moreover, the shoulder of the pin tool plays a very important role in the welding process [17]. Mathematical models have been made to develop the equations for thermal conductivity, density, and specific heat and their relationship with the maximum temperature generated by friction when performing the friction stir welding process, and the theoretical results are in an acceptable agreement with the practical results [18]. Models were designed and tested to study the heat flux resulting from friction during friction stir welding, and the results showed that (95%) of the heat is transmitted to the model and the rest (5%) leaks into the welding tool [19]. The quality of welding was studied during friction stir welding, where welding was carried out using nine models, and three different rotational speeds were used for the welding tool, plus three different travel speeds for the trolley carrying the models [20]. The behavior of friction stir welding for aluminum alloy (AA6061-T6) was studied using four rotational speeds of a welding pen. Heat output was measured with built-in thermocouples in study areas with limited welding implemented element model using ANSYS 12.1 package graphics, further results are shown. Measurements of the maximum temperature in this case is 0.71 of the temperature of the liquefied sample, at the maximum rotational speed of 1450 rpm [21].

The researchers studied a two-dimensional model on an aluminum alloy on the basis of finite element analysis. The model mechanically integrates the interaction of the tool and the thermomechanical process of the welded material. The calculation result also shows that the workpiece preheats before the FSW process. Welding parameters such as preheating (100, 200), rotating speed (960, 1200 rpm) and travel speed (110, 155, 195 mm/min), was found to be beneficial to increasing the working temperature in front of the pin tool, making the material easy to weld. There is no need to use high values for revolution speed or travel speed with preheating process [22]. The researchers developed digital solutions using the Finite Element Method (FEM) based on the ANSYS program for W-AA2024 aluminum alloy. These solutions have been developed based on the relationship between the properties of thermal conductivity, specific heat, and density, as these properties change with the shift of degrees of heat. The obtained simulations were practically verified and the comparative results were in agreement [23].

Methods for improving the mechanical properties of samples that are welded by friction stir at different rotational speeds of the welding tool and at a constant travel speed were studied in order to transform the heterogeneous microstructure into a more homogeneous microstructure, where the best results were obtained when using the travel speed of 60 mm/min and the rotational speed of 130 rpm, which reached welding efficiency of 84.61% [24]. The heat transfer was studied in an aluminum plate (AA-6061) welded by friction stir, where a theoretical and practical study was conducted, and three types of welding tools were used (triangular, cylindrical and conical). The results showed that the highest temperature distribution was achieved when using the conical welding tool and the reason for this is determined by the high torque and axial load, and the theoretical results are in agreement with the experimental results [25].

A mathematical model was done by finite element method in order to study the heat lane during the friction stir welding process by understanding the physical phenomena, using aluminum sheets (T53-7020) and using four different travel speeds for the welding tool. The results showed that the temperatures on the advanced side are higher than those on the retreating side and the practical results were in agreement with the theoretical results, where the highest welding temperature reached 70% of the melting temperature of the original metal Also, the authors studied the influence of friction stir welding coefficients on temperature distribution and tensile strength of aluminum alloy (6061-T6) [26].

Four different rotations of the welding tool and a constant travel speed of the trolley carrying the model are used. Consequential mechanical tests showed that using a speed of 500 rpm and 14 mm/min gives the best strength [27]. The researchers prepared an alloy AA6061–T3 AA2024 exposed to steel balls with a diameter of 25.1 mm for a period of 15 minutes at a welding speed of 56, 40, 28 mm/min with the rotational speed fixed at 1400 rpm. The welding speed of 40 mm/min and the same rotational speed of 1400 rpm were selected in the process of welding the plates that were extruded to show the effect of the extrusion

process on mechanical properties. There was a decrease in the mechanical properties when increasing the travel speed and a better result appeared at a travel speed of 28min/mm when the process of throwing steel balls before the welding process contributed to improving the mechanical properties to a certain degree. An approach to the results of the base metal shows that there was an improvement in the mechanical properties when increasing the rotational speed [28]. Welded models were tested using the aluminum alloy (AA-7008) and the friction stir welding method, at different rotational speeds of the welding tool. It was found that the rotational speed of the welding tool has a key role in increasing the generated temperatures and the amount of heat transferred during the welding process [29], [30].

In the paper, the authors focus on the study of the temperature distribution in two aluminum alloys (2024 - T3 and 7075 - T6) joined by friction stir welding, by changing the rotational speed of the welding tool, the travel speed of the process, and also by building a mathematical model to predict temperatures on all points of the two welded surfaces.

2. MATERIALS USED

Two types of aluminum alloys were used to join them by using friction stir welding process (AA7075–T6 & AA2024–O). These dissimilar alloys are difficult to join by traditional methods. Table 1 shows the chemical composition of the alloys approved by the European Aluminum Association (EAA), while table 2 shows the mechanical specifications of the alloys used in this study, according to the American specifications (ASTME 3-01) [31]. Table 3 shows the thermal properties of the aluminum alloys.

Table 1. The chemical composition of aluminum alloys [32]

Elements Materials	Zn %	Si %	Fe %	Cu %	Mn %	Mg %	Cr %	Ti %	Al %
Actual Chemical Composition, AA-2024 – O	0.21	0.33	0.41	4.33	0.63	1.51	0.08	0.13	92.26
Actual Chemical Composition, AA-7075 – T6	5.4	0.5	0.15	1.9	0.3	2.54	0.25	0.2	88.76

Table 2. Mechanical properties of aluminum alloys [33]

Aluminum Alloy	Density, Kg/m³	Tensile Yield Strength MPa	Ultimate Tensile Strength MPa	% EL	Modulus of Elasticity, GPa	Shear modulus, GPa	Hardness, Vickers	Hardness, Brinell	Poisson ratio
Nominal value, AA- 2024 – O	2780	345	483	10	73.1	28	137	120	0.33
Nominal value, AA-7075 – T6	2810	503	572	11	71.7	26.9	175	150	0.33

Table 3. Thermal properties of aluminum alloy [33]

Aluminum Alloy	CTE, Travel 205, c°	Specific heat capacity, $\frac{j}{g.c^{\circ}}$	Thermal conductivity, $\frac{W}{m.c^{\circ}}$	Melting point, c°
Nominal value, AA- 2024 – O	24.7	0.875	121	638
Nominal value, AA-7075 – T6	52.5	0.96	130	635

3. NUMERICAL MODELING

Two aluminum alloys plates were used for the study, having the dimension of 100×100×5mm. The ANSYS 15.0 program was used to analyze the temperature distribution on the surfaces of the two plates joined by friction stir welding process, using finite element method. In the model, the thermo-physical parameters were introduced, and the geometrical model was achieved, as shown in figure 1.

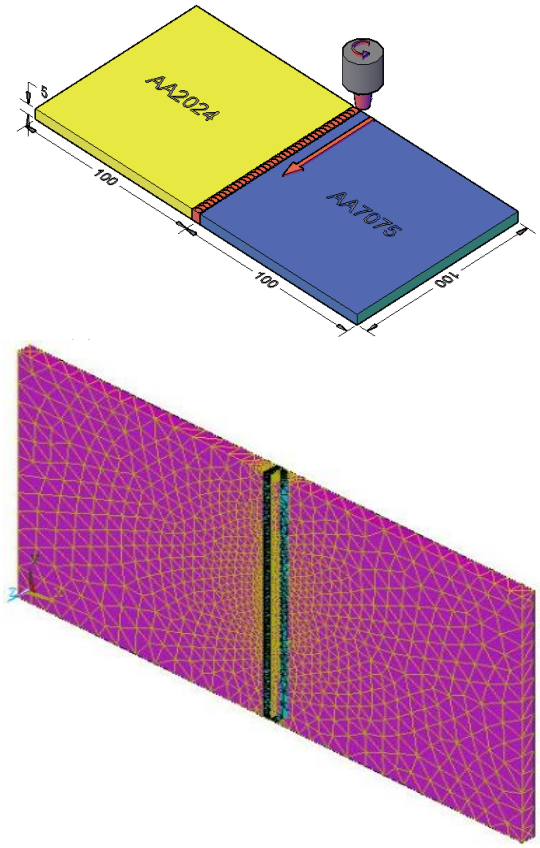

Fig. 1. Isometric view of the geometrical model

Figure 2 depicts the steps in working with the software used in this study. The program is firstly opened and thermal analysis is selected. After, the geometrical model is designed for the plate of the first alloy, the plate of the second alloy, and finally the third material in between them, that is considered the weld. After creating the connection between the models, the thermo-physical and mechanical proprieties are introduced, for each alloy, as well as for the weld, whose specifications are a combination

of the specifications of the two alloys. After, the geometrical model is divided into infinitesimal pieces, in accordance with the analysis of the finite element method.

After this step, the loads must be introduced defined, and finally, the selection of a solution is made, in order to solve the program and arrive at the desired results.

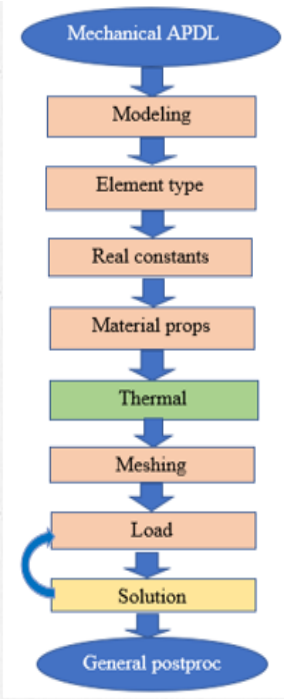

Fig. 2. Steps for implementing the mathematical model in ANSYS 15.0.

Table 4 shows the values of the variables that were used as boundary conditions, changing the tool's rotational speed for each value of the travel speed (TS). While the values of the variables used as a boundary condition are shown in table 3, the travel speed of the work piece (TS) changes as a function of the tool's rotational speed (TRS).

Table 4. Boundary conditions and different rotational speed (TRS)

No.	Travel speed, (mm/min)	Welding time, (Sec.)	Shoulder diameter, (d, mm)	rotation speed, (rpm)	Temperature, C°		Model
					Max.	Min.	
1	20	300	17.5	900	453	25	1
				1050	466	25	2
				1200	472	25	3
2	40	150	17.5	900	444	25	4
				1050	457	25	5
				1200	463	25	6
3	60	100	17.5	900	431	25	7
				1050	444	25	8
				1200	450	25	9
4	100	60	17.5	900	405	25	10
				1050	418	25	11
				1200	424	25	12

Table 5. Boundary condition and different travel speed (TS)

No.	Tool rotation speed, (rpm)	Shoulder diameter, (d, mm)	Travel speed, (mm/min)	Welding time, (Sec.)	Temperature, C°		Model
					Max.	Min.	
1	900	17.5	20	300	453	25	13
			40	150	444	25	14
			60	100	431	25	15
			100	60	405	25	16
2	1050	17.5	20	300	466	25	17
			40	150	457	25	18
			60	100	444	25	19
			100	60	418	25	20
3	1200	17.5	20	300	472	25	21
			40	150	463	25	22
			60	100	450	25	23
			100	60	424	25	24

4. AREAS WHERE THE MODELS WERE COMPARED

In order to compare the models and the temperature distribution on the surfaces of the two alloys, joined by friction stir welding process, from the center of the welding area and the advanced side of the welding of the alloy (AA-7075-T6), to the regressive side of the aluminum alloy (AA-2024-O) on the upper surface, the areas in which the results of the tests were determined in the ANSYS 15.0 program are shown in figure 3.

Figure 3 depicts the designated areas from the start of welding to the end, in order to understand the link between temperature and time. It also depicts the designated areas from the welding center to the alloy margins, analyzed in order to understand the relationship between temperatures and distance.

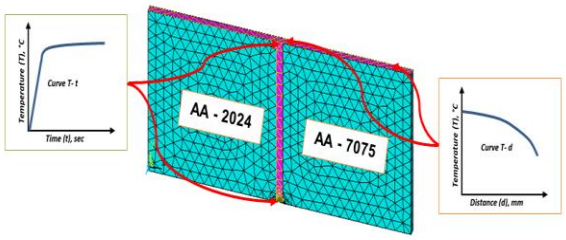

Fig. 3. The selected areas for the temperature distribution prediction after the welding process

5. RESULTS AND DISCUSSION

5.1. Effect of Tool Rotational Speed

In order to investigate the outcomes on the upper horizontal surface of welded alloys (AA7075-T6 and AA2024-O), in case of different tool rotational speeds (TRS = 900, 1050, 1200 rpm), the rotational speeds were adjusted while the travel speeds were left constant. Figure 4 demonstrates that when the tool's rotational speed at constant travel speed increase, the temperatures from the welding center to the two ends

of the model do as well. The greatest values were recorded when the tool's rotational speed was TRS=1200 rpm.

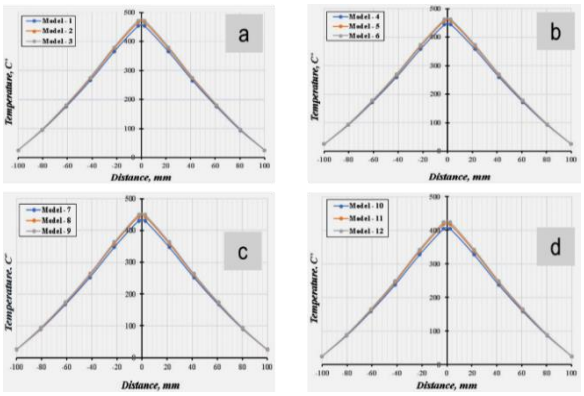

Fig. 4. Temperature vs. distance along the weld line on the top surface:
a) TS=20mm/min; b) TS=40 mm/min;
c) TS=60 mm/min; d) TS= 100mm/min

In figure 5 are presented the reached temperature achieved at different travel speeds with various rotational speeds of the welding equipment, and the findings reveal that the third model, had the maximum temperature with the travel speed of 20 mm/min and rotational speed of 1200 rpm. This is caused by two factors: first, the increased rotational speed and, second, the lengthened welding process.

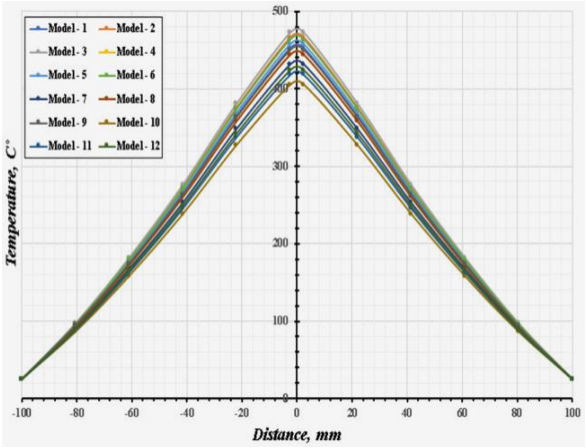

Fig. 5. Temperature vs. distance on the upper horizontal surface for welded alloys for TS = 20, 40, 60, 100 mm/min

The distribution of temperatures over the entire welded specimen is shown in figure 6, reached using a constant travel speed of TS = 20 mm/min and different rotational speeds.

From the figure 6 it can be observed that the third model's surface, had the highest temperatures for TS = 20 mm/min and TRS = 1200rpm (Fig. 6c).

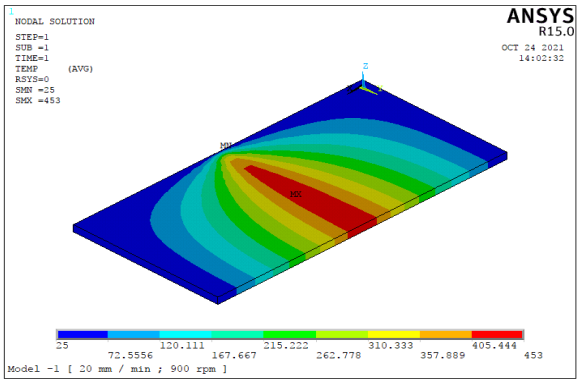

a)

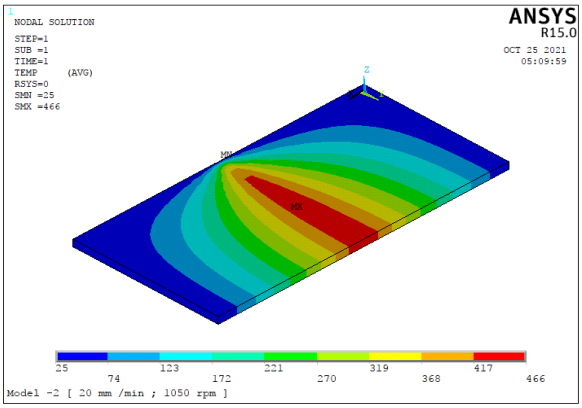

b)

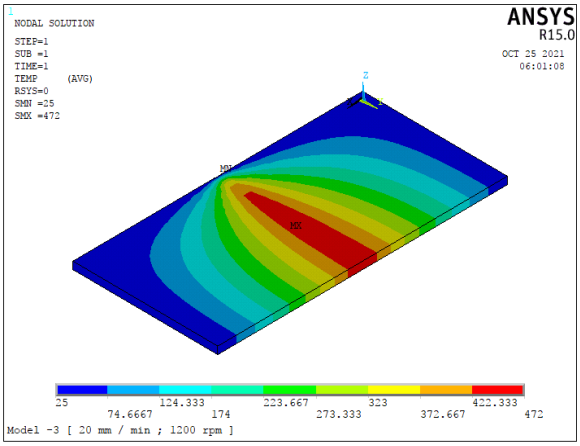

c)

Fig. 6. The temperature distribution on the surface of the model for: a) TRS=900 rpm; b) TRS=1050 rpm; c) TRS=1200 rpm and TS =20 mm/min

.

The distribution of temperatures over the entire welded specimen is shown in figure 7, with a constant travel speed of TS = 40 mm/min and different rotational speeds. From the figure it can be observed that the third model's surface had the highest temperatures for TS = 40 mm/min and RS = 1200rpm.

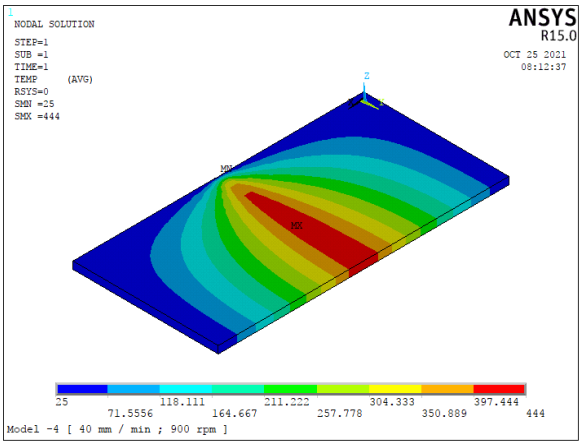

a)

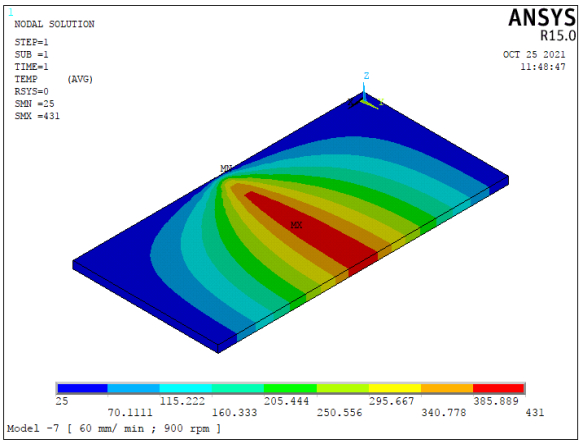

a)

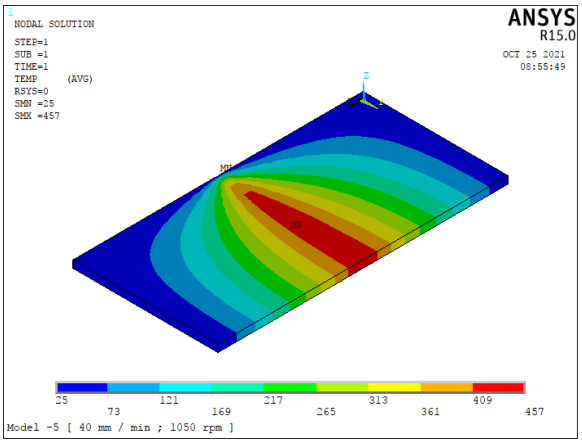

b)

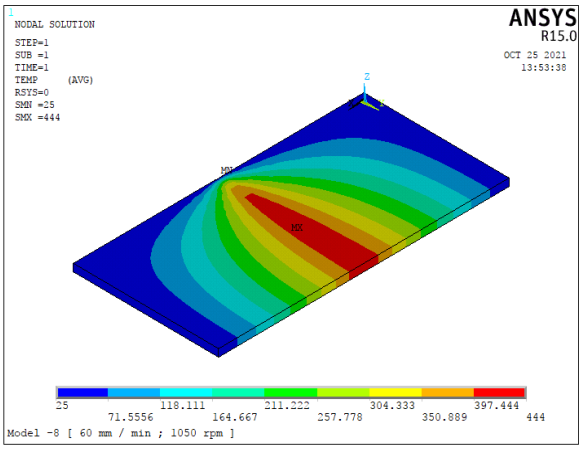

b)

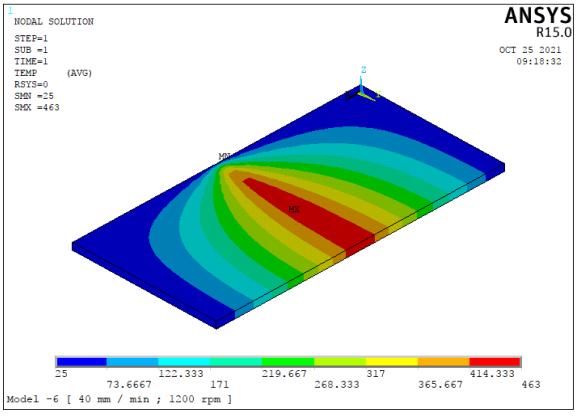

c)

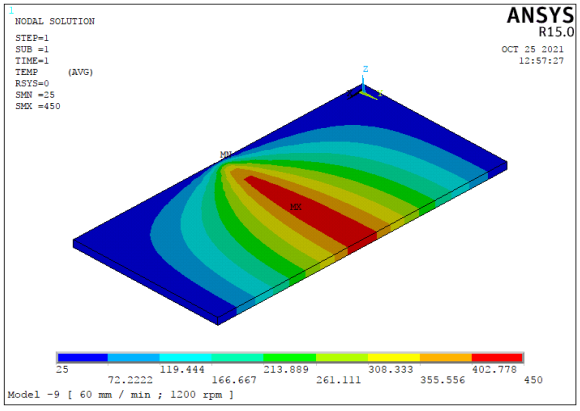

c)

Fig. 7. Temperature distribution on the surface of the model when: a)TRS=900 rpm; b) TRS=1050 rpm; c) TRS=1200 rpm and TS =40 mm/min

Fig. 8. The temperature distribution on the surface of the model when: a) TRS=900 rpm; b) TRS=1050 rpm; c) TRS=1200 rpm and TS =60 mm/min

.

The distribution of temperatures over the entire welded specimen is shown in figure 8 with a constant travel speed of TS = 60 mm/min and different rotational speeds. In the figure it can be observed that the third model's surface had the highest temperatures, for TS = 60 mm/min and TRS = 1200 rpm.

Figure 9 shows the distribution of temperatures over the entire welded specimen at different rotating speeds and a constant travel speed of TS = 100 mm/min). From the figure it can be observed that the third model's surface had the highest temperatures, for TS = 100 mm/min and RS = 1200 rpm.

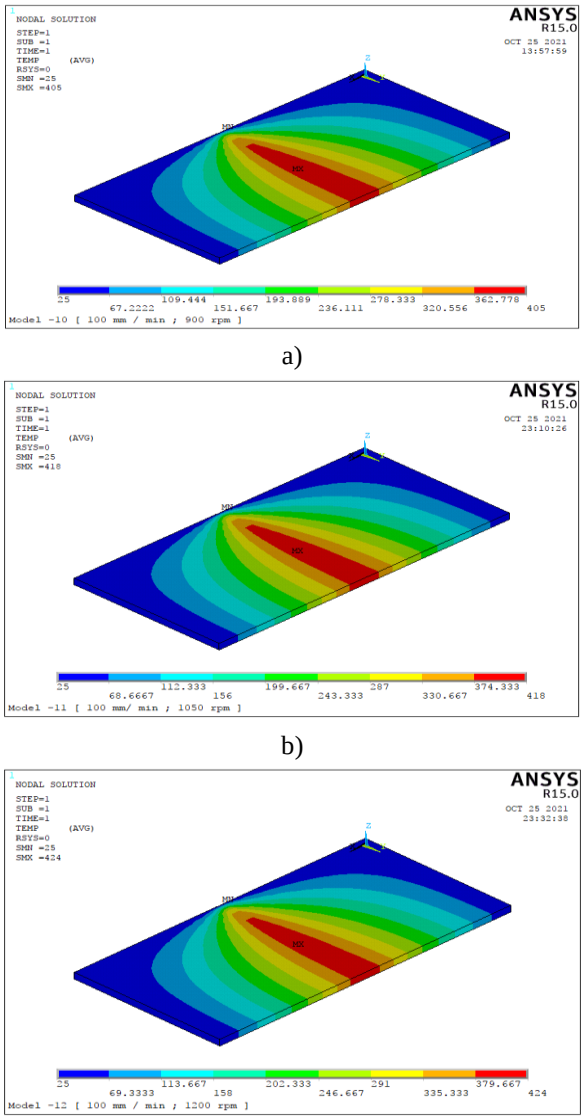

Fig. 9. Temperature distribution on the surface of the model for: a) TRS=900 rpm; b) TRS=1050 rpm; c) TRS=1200 rpm and TS =100 mm/min

5.2. Effect of Welding Speed

Figure 10 shows the temperature distributions, in cross sections, druing the friction stir welding process of the aluminum alloys AA7075-T6 and AA2024-O, at different travel speeds of TS = 20, 40, 60, 100 mm/min). This graph shows the impacts of stabilizing the welding tool's rotational speed and altering the travel speed of the cart carrying the models, as the temperatures of the models increses with time. The temperature was highest when the rotational speed (TRS) and travel speed (TS) were equal to 1200 rpm.

Figure 11 combines different travel speeds of the vehicle carrying the models of TS = 20, 40, 60, 100mm/min) with different rotational speeds of the welding tool, respectively RS = 900, 1050, 1200 rpm. The findings indicate that the twenty-one model, with the welding tool's rotational speed of RS = 1200 rpm and the model's travel speed of TS=20 mm/min, had the maximum temperature.

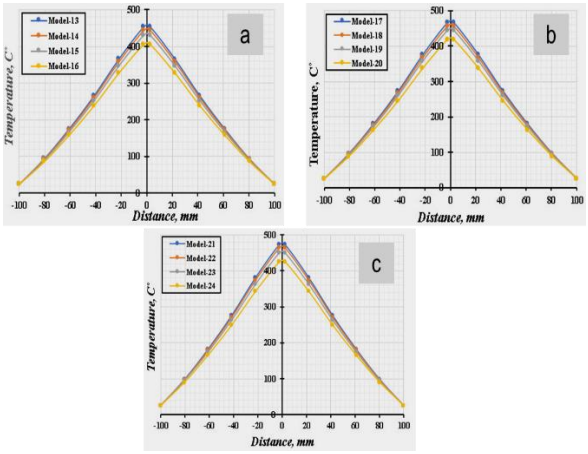

Fig. 10. Temperature vs. distance along the weld line on the top surface: a) TRS=900rpm; b) TRS=1050rpm; c) TRS=1200rpm

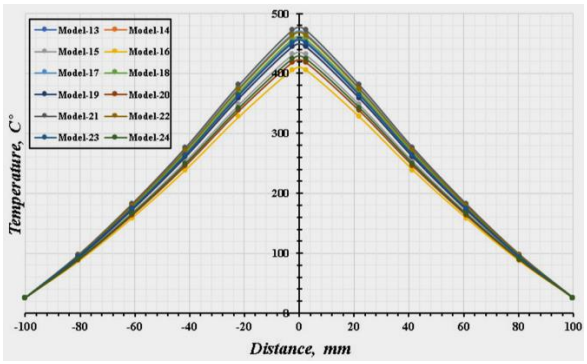

Fig. 11. Temperature vs. distance along the weld line on the top surface, TRS=900, 1050, 100 rpm

Figure 12 depicts the distribution of temperatures across the entire welded specimen with the welding tool's constant rotational speed (TRS = 900 rpm) and the models' varying travel speeds (TS=20, 40, 60, 100 mm/min). The figure reveals that the thirteen models with the highest temperatures (TRS = 900 rpm & TS=20 mm/min) had their surfaces exposed.

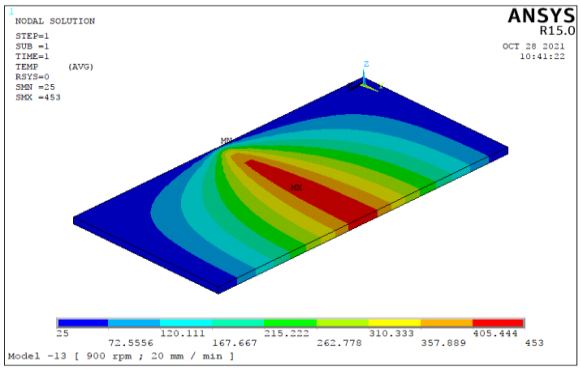

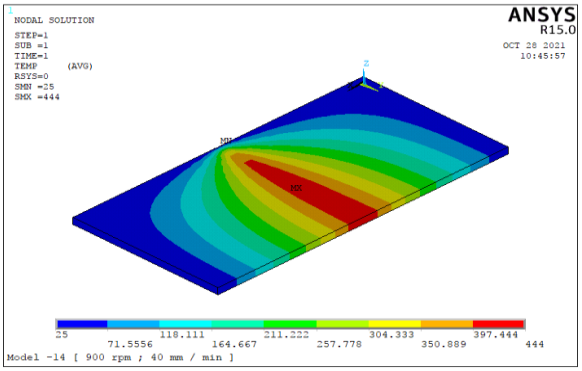

b)

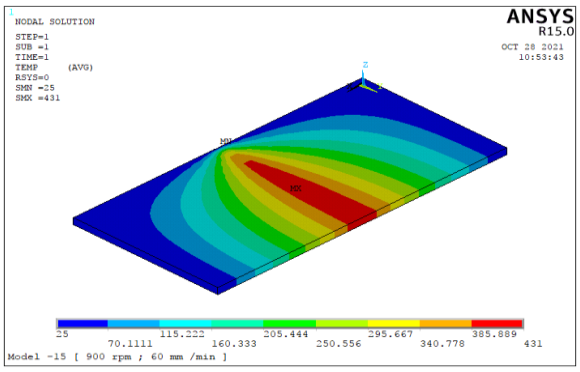

c)

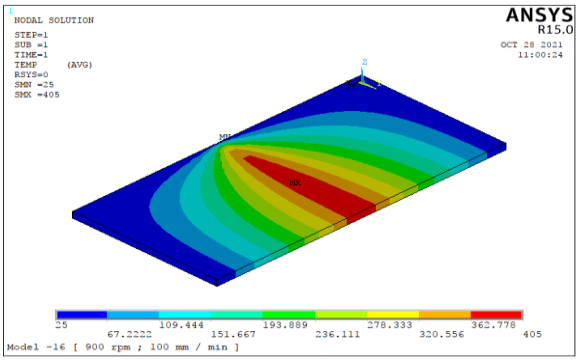

d)

Fig. 12. The temperature distribution on the surface of the model for: a) TS=20 mm/min; b) TS=40 mm/min; c)TS=60 mm/min; d) TS=100 mm/min and TRS =900 rpm

Figure 13 shows the distribution of temperatures across the whole welded specimen with varying model travel speeds, respectively TS=20, 40, 60, 100 mm/min, and a constant welding tool rotation speed of TRS = 1050 rpm. The graph shows that surfaces of the seventeen models have the greatest temperatures for TRS = 1050 rpm and TS = 20 mm/min.

Figure 14 shows the temperature distribution across the entire welded specimen with the models moving at different speeds, respectively at TS = 20, 40, 60, 100 mm/min, and the welding tool rotating at a constant speed of TRS = 1050 rpm, with a twenty-one-model, having the highest temperatures at TRS = 1200 rpm and TS = 20 mm/min.

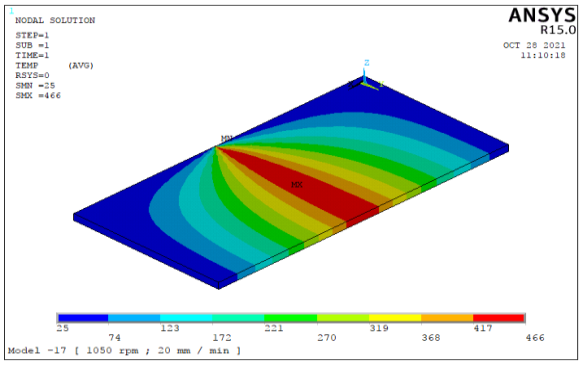

a)

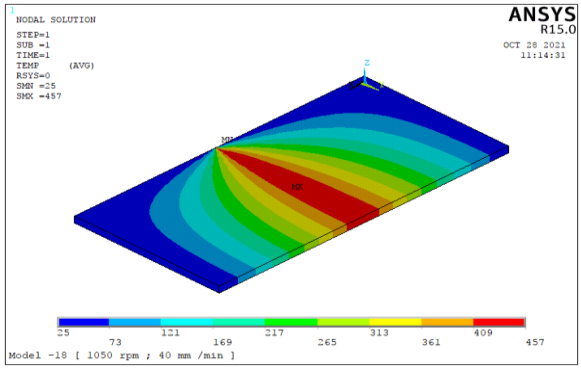

b)

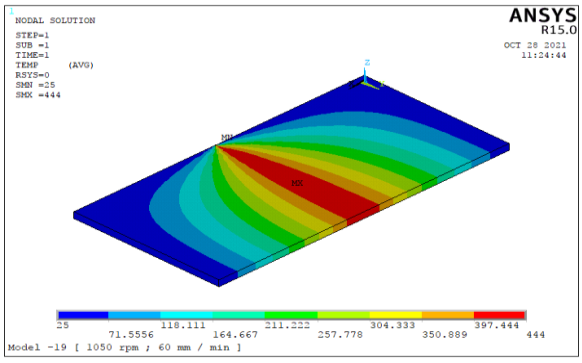

c)

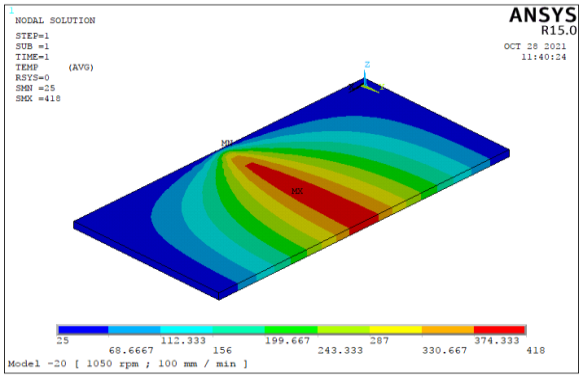

d)

Fig. 13. The temperature distribution on the surface of the model for: a) TS=20 mm/min; b) TS=40mm/min; c) TS=60 mm/min; d) TS=100 mm/min and TRS =1050 rpm

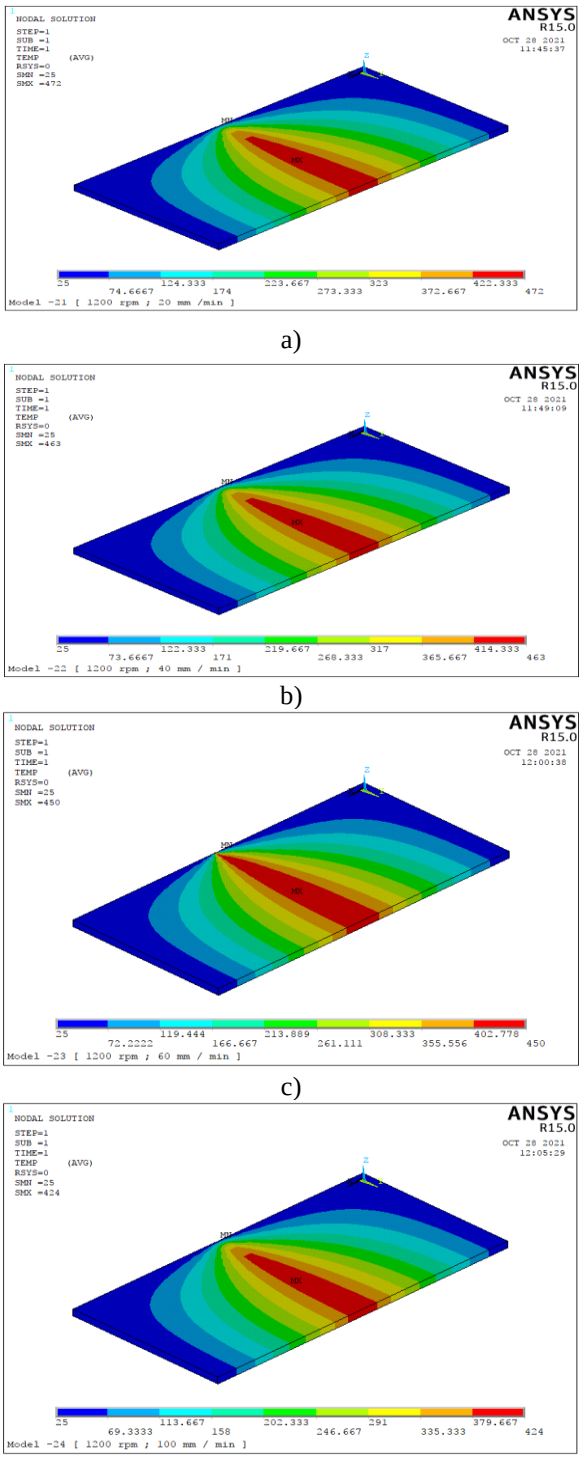

Fig. 14. The temperature distribution on the surface of the model when: a) TS=20 mm/min; b) TS=40 mm/min; c) TS=60 mm/min; d) TS=100 mm/min and TRS =1200 rpm

5.3. Effect of Welding Speed by Stabilizing the Rotational Speed and Changing the Travel Speed

Figure 15 illustrates the findings and the relation between the length of time required for the welding process, from the start to the finish, and the temperatures on the welding center at various model travel speeds of TS = 20, 40, 60, 100 mm/min, and the rotational speed of the welding tool at of TRS=900, 1050, 1200 rpm. The results in figure 14a clearly show that the temperatures reached maximum when the rotational and travel speeds were respectively set at 1200 rpm and 20 mm/min. The model in figure 14b with the welding tool rotating at TRS=1200 rpm, and the car transporting the model traveling at TS=40 mm/min had the highest temperatures. The figure 14c illustrates that, from the start of the welding process to its end, the maximum temperatures occurred at travel speeds of TS=60 mm/min and rotational speeds of TRS=1200 rpm. The model in figure 14d with the fastest travel speed of TS=100mm/min, and welding tool rotating speed of TRS=1200rpm had also the greatest temperatures.

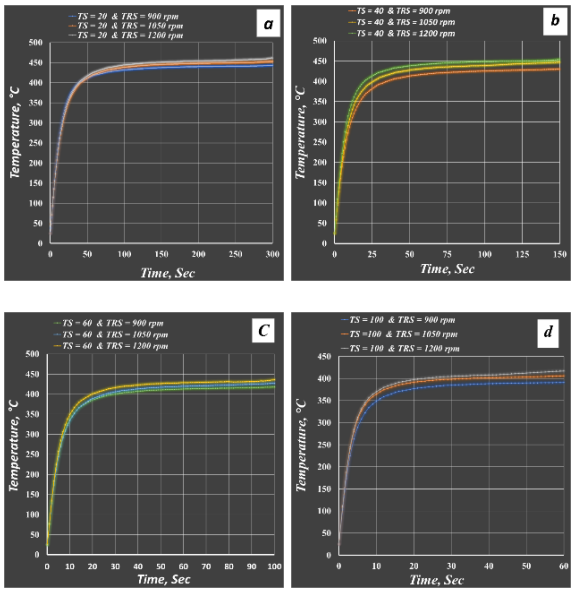

Fig.15. Temperature vs. time during the welding process for: a) TS = 20 mm/min; b) TS = 40 mm/min; c) TS = 60 mm/min; d) TS = 100 mm/min

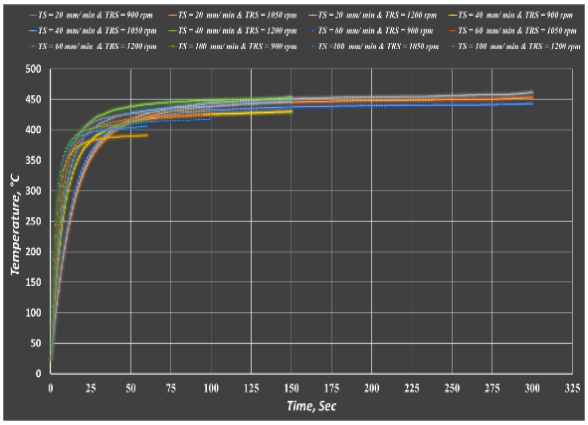

Fig. 16. Temperature vs. time during the welding process for TS = 20, 40, 60, 100 mm/min

In figure 16, different travel speeds (TS = 20, 40, 60, 100 mm/min) and different rotational speeds of the welding tool (TRS = 900, 1050, 1200 rpm) are compared to the time spent in the welding process, from the beginning to the end, and the temperature distribution of the model, from the starting point of the welding process to its end is shown. The graph demonstrates that the increase in the model's travel speed is greater in the first twenty-five seconds, but that it afterwards declines as a result of the welding process taking less time for models of the same length.

5.4. Effect of Welding Speed by Stabilizing the Travel Speed and Changing the Rotational Speed

The outcomes of the time spent building the models at a constant rotating speed and a varied travel speed at each rotational speed are shown in figure 17.

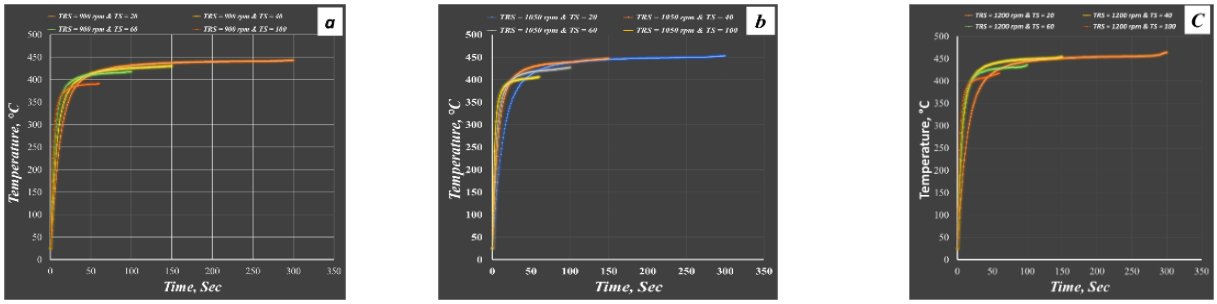

Fig. 17. Temperature vs. time during the welding process for: a) TRS=900 rpm; b) TRS=1050 rpm; c) TRS=1200 rpm

Figure 15a depicts the variation between the length of time spent welding the models at different travel speeds of TS = 20, 40, 60, 100 mm/min, and welding tool rotational speeds of TRS=900 rpm. The welded model with a rotating speed of TRS=900 rpm, and travel speed of TS=20 mm/min, at time of 50 sec until the end of the welding process, was found to have the greatest temperatures. The highest temperature distribution was for the model at a travel speed of TRS = 1050 rpm, and a rotation speed of TS = 20 mm/min, at 150 sec. until the welding process was complete, according to figure 15b, which depicts the relationship between time and temperature distribution at rotational speed at TRS = 1050 rpm, and travel speed of TS = 20, 40, 60, 100 mm/min. As for figure 15c, it displays the results of the welding process for models at different travel speeds of TS = 20, 40, 60, 100 mm/min, and rotational speeds of TRS=1200 rpm. The distribution of temperatures is shown along with the amount of time spent in the welding process, and the highest temperatures were achieved when welding the model at these speeds after 150 seconds.

For different rotational speeds of the welding tool, respectively of TRS = 900, 1050, 1200 rpm, and different travel speeds of TS = 20, 40, 60, 100 mm/min, figure 18 illustrates the relationship between the time spent during the welding process, from the beginning of the welding to its end, and the temperature distribution on the model from the starting point of the welding process to its end. According to the findings, which are depicted in the image, there was a discernible rise in temperature at constant travel speed as well as an increase in rotational speed. The temperatures produced during the welding process increase with the welding tool's spinning speed.

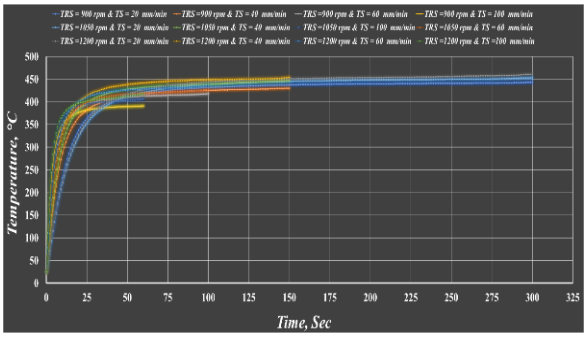

Fig. 18. Temperature vs. time during the welding process for TRS = 900, 1050, 1200 rpm

5.5. Equation for the Prediction of Temperature Distribution vs. Distance

Using the ANSYS-15.0 program for different rotational speeds of the welding tool of TRS = 900, 1050, 1200 rpm, and various travel speeds of TS = 20, 40, 60, 100 mm/min, the temperature distribution was taken along a line, from the center of the weld to the end of the model, consisting of (19 - A) shaped (AA-7075), and (19 - B) for the second plate (AA-2024). Using the Curve Expert program, a new equation was developed, to predict the temperature distribution. Several equations were tried, in order to find the most accurate one to predict the model's temperature in respect to the weld center's distance. Two equations were obtained, equation (1) for alloy (AA - 7075) and equation (2) for alloy (AA - 2024):

$$T = 0.0002668\ (1.0167896 - e^{0.0001621\ d}) \qquad (1)$$

$$T = 0.0002659\ (1.0168477 - e^{0.0001627\ d}) \qquad (2)$$

where T is temperature in [C°]; d – distance [mm].

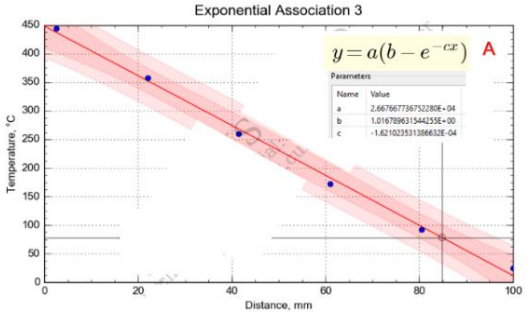

a)

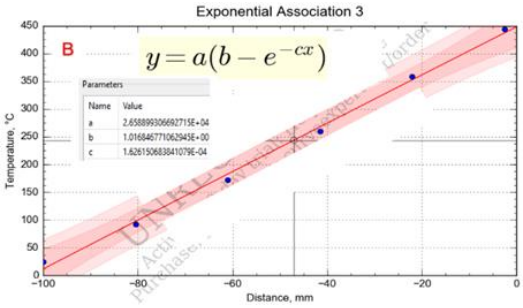

b)

Fig. 19. Model for the prediction of temperature distribution vs. distance: a) AA - 7075 alloy; b) AA – 2024 alloy

5.6. Equation for the Prediction of Temperature distribution vs. Welding Time

Using the ANSYS - 15.0 program, at various travel speeds of the cart transporting the model, respectively at TS = 20, 40, 60, 100 mm/min, and different tool rotational speeds of TRS = 900, 1050, 1200 rpm, the temperature distribution was taken on a longitudinal line, in the center of the weld, from the start of the welding process to its end. The average temperature distribution was then extracted over the longitudinal line using the Excel program. Using the Curve Expert program, a new equation was created to predict the distribution of temperatures along the welding line, from the start of welding to its end, versus the time required for the process.

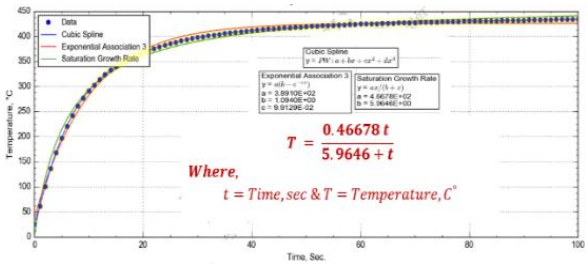

Fig. 20. Model for the prediction of temperature distribution vs. welding time

Several models of equations were tried to find the most accurate model that predict the temperature's distribution versus welding time. Figure 20 depicts the procedure that was used to arrive at the following equation:

$$T = \frac{0.46678\ t}{5.9646 + t} \qquad (3)$$

where T is temperature in [C°]; t – time [s].

6. CONCLUSIONS

The following conclusions can be summarized:

1. The temperature increases with the increase in the rotational speed of the welding tool, and the highest degrees are in the welding center and decrease as move away from the welding center.
2. The temperatures decrease with the increase of the travel speed of the welding cart, because the time taken in the welding process is shorter.
3. Equations for temperature prediction have been developed, where the two equations (1 and 2) show the prediction of temperature from the weld center to the edges of the two alloys, which is a relationship between temperatures and the distance from the weld center, while the equation (3) was developed to predict the temperatures in the weld center, from the beginning of the welding process to its end, and the equation is a relationship between the temperatures and the time of the welding process.
4. The temperature distribution is similar in both alloys (AA02024 & AA-075), due to the similar properties of both alloys, and the equations that were developed to predict the temperatures of the two alloys proved this conclusion (1 and 2).
5. The highest temperature was recorded in the twentieth second from the start of the welding process, and its value is 410ºC, at the travel speed of TS = 40 mm/min, and the rotational speed of the welding tool of RS = 900, 1050, 1200 rpm.

7. FUTURE RESEARCH DIRECTIONS

This work can be continued, as there are various studies to identify them and continue to address the problems of friction stir welding, below is a list the most important recommendations and future work:

I. Studying the effect of changing the concavity of the welding tool on welding efficiency, at different travel and rotational speeds, and using different welding tools.

II. Studying the effect of the initial heating of the welding tool on welding efficiency by using different welding tools and the different travel and rotational speeds.

III. Developing a mathematical model in the manner of the specified elements, to link the practical results obtained with the results that will be obtained from the mathematical models and compare them.

IV. Using two different alloys, one of which is aluminum and the other of copper, and joining using friction stir welding, using different tools, and different travel and rotational speeds, to identify the welding efficiency between the two alloys and to identify the weaker one.

V. Studying the effect of welding tool on welding efficiency, by using different types of welding tools and different travel and rotational velocities and comparing them.

ACKNOWLEDGMENTS

This research was supported by Engineering Science Research Program through the Northern Technical University / Ttechnical Engineering college and Technical Institute of Mosul funded by the Ministry of Higher Education and Scientific Research / Republic of Iraq. (No. 00233- 2021).

REFERENCES

[1] **Mishra R.S., Ma Z. Y.,** *Friction stirs welding and processing. Materials Science and Engineering*, R: Reports, 2005, vol. 50, iss. 1 -2, pp. 1 -78.

[2] **Nandan R., Debroy T., Bhadeshia H.K.D.H.,** *Recent advances in friction-stir welding - Process, weldment structure and properties*, Progress in Materials Science, 2008, vol. 53. iss. 6, pp. 980-1023.

[3] **Fuller C. B., Murray W. Mahoney, Calabrese M., Micona L.,** *Evaluation of microstructure and mechanical properties in naturally aged 7050 and 7075 Al friction stir welds*, Journal of Materials Science and Engineering, 2009, pp. 2233-2240.

[4] **Ciro Bitondo, et. al.,** *Friction-Stir Welding of AA 2198 butt joints: Mechanical Characterization of The Process and of The Welds Through DOE Analysis*, International Journal of Advanced Manufacturing Technology, 2011, vol. 53, pp.505–516.

[5] **Karash E. T. B., Yassen S. R., Kassim M. T. E.,** *Effect of friction stir welding parameters on the impact energy toughness of the 6061-t6 aluminum alloys*, Annals of "Dunarea de Jos" University, Fascicle XII, Welding Equipment and Technology, 2018, vol. 29, pp. 27-32.

[6] **Bušić M., Kožuh Z., Klobčar D.,** *Influence of the tool travel speed on friction stir processing of aluminum alloy alcu4mg1*, Annals of "Dunarea de Jos" University, Fascicle XII, Welding Equipment and Technology, 2017, vol. 28, pp. 11-14.

[7] **Birsan D., Scutelnicu E.,** *Modelling of thermo-mechanical effects generated by friction spot stir welding process*, Annals of "Dunarea de Jos" University, Fascicle XII ISSN 1221-4639 Welding Equipment and Technology, 2014, Vol. 25. pp. 29-34.

[8] **Birsan D., Scutelnicu E., Stan F.,** *Hardness of friction stir welded joints of AA-6061-t6 aluminum alloy*, Annals of "Dunarea de Jos" University of Galati Fascicle XII, Welding Equipment and Technology, 2010, vol. 21.

[9] **Rusu C. C., Mistodie L. R.,** *Thermography used in friction stir welding processes*, Annals of "Dunarea de Jos" University of Galati, Fascicle XII, Welding Equipment and Technology, 2010, vol. 21.

[10] **Birsan D., Iordachescu D., Ocana J. L., Vilaca P.,** *FEM model for Friction Stir Welding of Aluminum*, The Annals of "Dunarea de Jos" University of Galati, Fascicle XII, Welding Equipment and Technology, Year XIX, 2008.

[11] **Thomas W. M., et. al.,** *Friction Stir Butt Welding*, International patent application no. PCT/GB92/02203 and GB patent application no.9125978.8, 6 December 1991.

[12] **Rajakumar S., Muralidharan C., Balasubramanianet V.,** *Statistical Analysis to Predict Grain Size and Hardness of the Weld Nugget of Friction Stir-Welded AA6061-T6 aluminum alloy joints*, The International Journal of Advanced Manufacturing Technology, 2011, vol. 57, pp. 151–165, DOI 10.1007/s00170-011-3279-5.

[13] **Zhang Z., Zhang H. W.,** *Material Behaviors and Mechanical Features in Friction Stir Welding Process*, The International Journal of Advanced Manufacturing Technology, 2007, vol. 35, pp.86–100.

[14] **Palanivel R., et. al.,** *Development of Mathematical Model to Predict the Mechanical Properties of Friction Stir Welded AA6351 Aluminum Alloy*, Journal of Engineering Science and Technology Review, vol. 4, iss. 1, 2011, pp. 25-31.

[15] **Mohammad R., Hamidreza N.,** *Analysis of Transient Temperature and Residual Thermal Stresses in Friction Stir Welding of Aluminum Alloy 6061-T6 via Numerical Simulation*, The International Journal of Advanced Manufacturing Technology, 2011, vol. 55, pp.143–152.

[16] **Padmanaban R., Ratna Kishore V., Balusamy V.,** *Numerical Simulation of Temperature Distribution and Material Flow During Friction Stir Welding of Dissimilar Aluminum Alloys*, Procedia Engineering, 2014, vol. 97, pp.854-863.

[17] **Tang W., Guo X., Mcclure J. C., Murr L. E.,** *Heat Input and Temperature Distribution in Friction Stir Welding*, Journal of Materials Processing and Manufacture Science, 1998, vol. 7: pp.163-172

[18] **Prasanna P., Subba Rao B., Krishna Mohana Rao G.,** *Experimental and numerical evaluation of friction stir welds of aa6061-t6 aluminum alloy*, ARPN Journal of Engineering and Applied Sciences, 2010, vol. 5, pp.1-18.

[19] **Chao Y. J., Qi X., Tang W.,** *Heat Transfer in Friction Stir Welding—Experimental and Numerical Studies*, Transactions of the ASME, 2003, vol. 125, pp.138-145.

[20] **Shabbir M., Jacek T., Hesamoddin A. D.,** *Thermo-Mechanical Simulation of Underwater Friction Stir Welding of Low Carbon Steel*, Materials, 2021, vol. 14, 4953, pp. 2-17.

[21] **Peel M.J., Steuw Er A., Withers P.J., Dickerson T., Shi Q., Sher Cliff H.,** *Dissimilar Friction Stir Welds in AA5083-AA6082.Part I: Process Parameter Effects on Thermal History and Weld Properties*, Metallurgical and Materials Transactions A, 2006, vol. 37a, pp. 2183-2193.

[22] **Abed R. N.,** *Influence of Friction Stir Welding Rotation Speeds In dwell phase on the Temperature Distribution of AA6061-T6 Aluminum Alloy Weldment*, Al-Nahrain Journal for Engineering Sciences (NJES), 2017, vol. 20, pp.719-726.

[23] **Doos Q. M., Zaidan A., Hassan R. Hassan.**, *Theoretical analysis of temperature distribution in friction stir welding*, Journal of Engineering, 2011, vol. 3, pp. 517-533.

[24] **Takhakh A. M., Shakir H. N.,** *Experimental and numerical evaluation of friction stirs welding of AA W aluminum alloy-2024*, Journal of Engineering, 2012, vol. 6, pp.717-734.

[25] **Ali A. A., Ayad M. T., Kadhim K. R.,** *Study the Mechanical Properties and Numerical Evaluation of Friction Stir Processing (FSP) for 6061-T6 Aluminum Alloys*, Al-Nahrain University, College of Engineering Journal (NUCEJ), 2016.19: p.255 – 264.

[26] **Mohsin N. H., Sadeq H. B., Mujtaba A. F.,** *Numerical and Experimental Investigations of Transient Temperature Distribution In Friction Stir Spot Welding Of Aluminum Alloy AA6061*, Al - Qadisiyah Journal for Engineering Sciences, 2016, vol. 9, pp.388-407.

[27] **Muhsin J. J., Moneer H. T., Muhammed A. S.,** *Theoretical and Experimental Investigation of Transient Temperature Distribution in Friction Stir Welding of AA 7020-T53*, Journal of Engineering, 2012, vol. 6, pp.693-709.

[28] **Majeed M. H.,** *Effects of Welding Parameters on Temperature Distribution and Tensile Strength of AA6061-T6 Welded by Friction Stir Welding*, Journal of Engineering, 2015, vol. 11, pp.24-39.

[29] **Hassan K. S.,** *Microstructural Characterization and Mechanical Properties of Similar and Dissimilar Al Alloys Joined using Friction Stir Welding*, Al-Khwarizmi Engineering Journal, 2018, vol. 14, pp. 19-28.

[30] **Kabir A. S. H., Cao X., Gholipour J., Wanjara P., Cuddy J., Birur, A., Medraj M.,** *Effect of postweld heat treatment on microstructure, hardness, and tensile properties of laser-welded Ti-6Al-4V. Metall*, Mater. Trans. A 2012, vol. 43, pp. 4171–4184.

[31] *** **ASTM** E 3 – 01. Standard Guide for Preparation of Metallographic Specimens, USA, 2001.

[32] *** **ASM** Aerospace Specifications Metals Inc. - retrieved 18 September 2019.

[33] *** **Alcoa 2024** data sheet Archived 2006-08-27 at the Way back Machine (pdf), accessed October 13, 2006.